Silicon-Organic Hybrid (SOH) and Plasmonic-Organic Hybrid (POH) Integration

C. Koos[1,2,*], J. Leuthold[3], W. Freude[1], M. Kohl[2], L. R. Dalton[4], W. Bogaerts[5], A.-L. Giesecke[6], M. Lauermann[1], A. Melikyan[2], S. Koeber[1,2], S. Wolf[1], C. Weimann[1], S. Muehlbrandt[2], K. Koehnle[2], J. Pfeifle[1], R. Palmer[1], D. Korn[1], L. Alloatti[1], D. L. Elder[4], T. Wahlbrink[6], J. Bolten[6]

[1]*Institute of Photonics and Quantum Electronics (IPQ), Karlsruhe Institute of Technology (KIT), 76131 Karlsruhe, Germany*
[2]*Institute of Microstructure Technology (IMT), Karlsruhe Institute of Technology (KIT), 76131 Karlsruhe, Germany*
[3]*Electromagnetic Fields and Microwave Electronics Laboratory, Swiss Federal Institute of Technology (ETH), Zurich, Switzerland*
[4]*University of Washington, Department of Chemistry, Seattle, WA 98195-1700, United States*
[5]*Photonics Research Group, Ghent University – imec, Gent, Belgium, and Luceda Photonics, Dendermonde, Belgium*
[6]*AMO GmbH, 52074 Aachen, Germany*
**email: christian.koos@kit.edu*

Abstract: Silicon-organic hybrid (SOH) and plasmonic-organic hybrid (POH) integration combines organic electro-optic materials with silicon photonic and plasmonic waveguides. The concept enables fast and power-efficient modulators that support advanced modulation formats such as QPSK and 16QAM.

OCIS codes: (250.7360) Waveguide modulators; (060.4080) Modulation; (230.7370) Waveguides; (250.5300) Photonic integrated circuits

1. Introduction: The need for hybrid integration

Silicon photonics offers tremendous potential for inexpensive high-yield photonic-electronic integration by leveraging fabless CMOS processing [1] - [5]. Besides conventional dielectric waveguides, plasmonic structures can also be efficiently realized on the silicon photonic platform, thereby reducing device footprint by more than an order of magnitude [6]. Silicon and metals, however, lack certain optical properties that are indispensable for high-performance photonic devices. In particular, neither of these materials exhibits appreciable second-order optical nonlinearities, thereby making efficient electro-optic (EO) modulators challenging. These deficiencies can be overcome by the concepts of silicon-organic hybrid (SOH) and plasmonic-organic hybrid (POH) integration, which combine silicon-on-insulator (SOI) waveguides and plasmonic nanostructures with organic electro-optic claddings. We give an overview on our recent progress in the field of SOH [6] - [21] and POH modulators [22], covering highly efficient devices with energy consumptions of a few femtojoules per bit, ultra-fast devices that enable modulation frequencies of up to 100 GHz, as well as advanced IQ modulators that are well suited for higher-order modulation formats such as quadrature phase-shift keying (QPSK) and 16-state quadrature amplitude modulation (16QAM).

2. Silicon-organic hybrid (SOH) integration

The basic structure of an SOH Mach-Zehnder modulator (MZM) is illustrated in Figure 1 (a) [7], [8]. The MZM comprises two SOH phase modulators that are driven in push-pull mode by a single coplanar transmission line in ground-signal-ground (GSG) configuration. Each of the phase modulators consists of a slot waveguide, which is covered by an organic EO material, see cross section in Figure 1 (b). The fundamental optical quasi-TE mode is strongly confined to the slot region due to field discontinuities at the slot sidewalls, Figure 1 (c). At the same time, the metal strips of the transmission line are electrically connected to the rails of the phase modulators by thin *n*-doped silicon slabs. A voltage applied to the transmission line drops across the narrow slot, resulting in a high modulation field that strongly overlaps with the optical quasi-TE mode [8], see Figure 1 (d). Logarithmically tapered strip-to-slot converters are used for coupling access strip waveguides to slot waveguides [9]. The π-voltages of our SOH MZM are obtained from measuring the transmission as a function of an applied DC voltage, see Figure 1 (e). For a device with 1.5 mm-long phase shifters, we find an π-voltage U_π of only 0.35 V for bias voltages of more than 2.9 V, corresponding to a voltage-length product of only $U_\pi L = 0.52$ Vmm, see Figure 1 (e) [10]. For smaller bias voltages, we observe increased spacings of the transmission dips and hence increased π-voltage, which is attributed to free ions in the cladding that lead to a partial screening of the applied fields at small bias voltages. This effect is only observable for low frequencies and does not impede RF operation. The modulation speed of the modulators is limited by the RC time constant of the slot waveguide: The slot corresponds to a capacitor which is charged and discharged via the resistive silicon slabs, see Figure 1 (d). The EO bandwidth can be increased by applying a static gate voltage between the substrate and the top silicon layer, which increases the conductivity of the slab by inducing a charge accumulation layer [8], [11]. Applying this technique to an ultra-short device of 500 µm length enables 3 dB bandwidths of more than 100 GHz, Figure 1 (f) [12]. In addition, we have shown that SOH waveguides with liquid crystal (LC) claddings enable particularly compact and power-efficient phase shifters – for a device length of 1.7 mm, we achieved an overall phase shift of approximately 80 π at a voltage of 4 V [19], [20].

3. Advanced electro-optic SOH devices: Modulation at fJ/bit and higher-order modulation formats

The performance of SOH devices can be boosted by using highly efficient cladding materials, featuring EO coefficients of up to 230 pm/V [10]. Combining these materials with ultra-short devices that can be operated as purely capacitive load, modulation energies of 10 fJ/bit and below have been demonstrated for conventional on-off keying

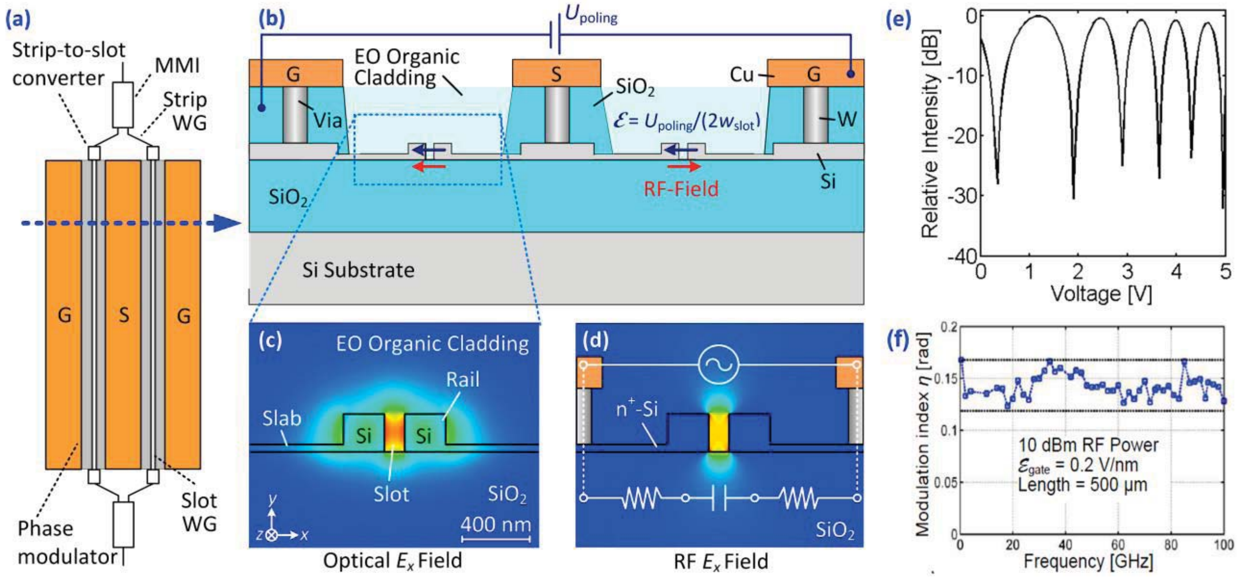

Figure 1: Silicon-organic hybrid (SOH) Mach-Zehnder modulator (MZM). (a) Schematic of the MZM. The device consists of two slot-waveguide (WG) phase modulators, driven in push-pull operation by a single coplanar ground-signal-ground (GSG) transmission line. (b) Cross-section of an SOH MZM based on tungsten vias that connect the GSG transmission line to the Si slot waveguide. Push-pull operation is obtained by an appropriate choice of poling directions (blue arrows) of the electro-optic (EO) cladding in both arms with respect to the direction of the local RF field (red arrows). (c) Cross-sectional view and simulated optical mode of a single phase modulator (slot width 160 nm, rail width 210 nm). The light is strongly confined to the slot due to electric-field discontinuities at the slot sidewalls. (d) Simulated RF mode field of the slot waveguide. The modulation voltage drops across the narrow slot resulting in a high modulation field that has a strong overlap with the optical mode. (e) Transmission vs. DC voltage of a MZM having 1.5 mm long phase shifters. At bias voltages above 2.9 V, the π-voltage of the device amounts to $U_\pi = 0.35$ V, corresponding to a voltage-length product of $U_\pi L = 0.52$ Vmm. For smaller DC voltages, free charges in the cladding lead to a partial screening of the applied electric field and hence to increased π-voltages. (f) High-speed modulation: Modulation index η vs. frequency for an on-chip RF power of 10 dBm. When using an electric gate field E_{gate} to increase the conductivity of the slabs, a 3 dB bandwidth of at least 100 GHz can be achieved [12]. The horizontal dotted black lines represent the maximum value and 70.7 % (–3 dB) thereof.

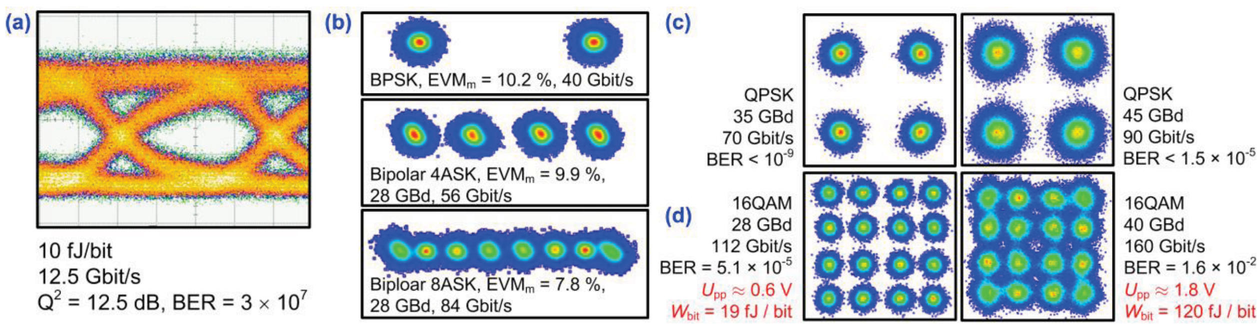

Figure 2: Experimental demonstration of high-performance SOH modulators. (a) Modulation at ultra-low energy consumption: When operating a short device with high electro-optic efficiency as a capacitive load, decent signal quality can be obtained for modulation energies as low as 10 fJ/bit [13]. (b) Constellation diagrams for BPSK and bipolar ASK along with the error-vector magnitudes (EVM). BPSK transmission was found to be error-free. For the bipolar 4ASK (56 Gbit/s) and the bipolar 8ASK (84 Gbit/s), the measured BER amounted to 2×10^{-6} and 9.7×10^{-3}, respectively [15]. (c) Constellation diagrams of QPSK signals for symbol rates of 35 GBd and 45 GBd [17], [18]. No bit errors were detected within our record length of 62.5 µs for 35 GBd, and the error vector magnitude (EVM_m) indicate error-free signals with BER < 10^{-9}. At 45 GBd, the BER amounts to 1.5×10^{-5} and is well below the threshold for hard-decision FEC with 7 % overhead. (d) Constellation diagrams of 16QAM-signals for symbol rates of 28 GBd and 40 GBd. For 28 GBd, the IQ modulator was operated with peak-to-peak voltages of $U_{pp} = 0.6$ V, leading to a power consumption of 19 fJ/bit and a BER of 5.1×10^{-5} - well below the threshold for second-generation hard-decision FEC. For 40 GBd, the BER is still below the 2.4×10^{-2} threshold for soft-decision FEC with 20 % overhead.

(OOK) at data rates of 12.5 Gbit/s, see Figure 2 (a) [13], [14]. Moreover, SOH Mach-Zehnder modulators are perfectly suited for data transmission with advanced modulation formats such as binary phase shift keying (BPSK) and bipolar amplitude shift keying (ASK), achieving data rates of up to 84 Gbit/s, Figure 2 (b) [15]. Quadrature phase shift keying (QPSK) and quadrature amplitude modulation (QAM) have also been demonstrated with symbol (raw data) rates of up to 45 GBd (90 Gbit/s) and 40 GBd (160 Gbit/s), Figure 2 (c) and (d) [16], [17], [18]. Including the FEC overhead, the raw data rate of 160 Gbit/s corresponds to a net data rate of 133 Gbit/s transmitted on a single polarization [18]. This is the highest value achieved by a silicon-based modulator up to now. For 16QAM transmission at 28 GBd, the IQ modulator was operated with peak-to-peak voltages of $U_{pp} = 0.6$ V, leading to a power consumption of 19 fJ/bit. This is the lowest drive voltage and the lowest energy consumption that have so far been reported for a 16QAM modulator in silicon [17].

4. POH devices: First proof-of-concept experiments

The speed limitations of SOH modulators can be overcome by plasmonic-organic hybrid (POH) devices, where both the optical mode and the RF signal are guided by metal pads, see Figure 3 [22]. The two pads form a metal slot waveguide in which light propagates as a surface plasmon polariton (SPP) mode. The slot is filled with an EO polymer, and phase modulation is achieved by applying a voltage to the metal sheets. As for silicon photonic slot waveguides, RF and optical field show perfect overlap in the EO cladding. Carrier relaxation in the metal pads occurs virtually instantaneously such that no RC limitations are to be expected. The viability of the device was demonstrated in a data transmission experiment using BPSK signaling at 40 Gbit/s. More recently, this principle was used to realize an ultra-small MZM operating at 72 Gbit/s BPSK [23].

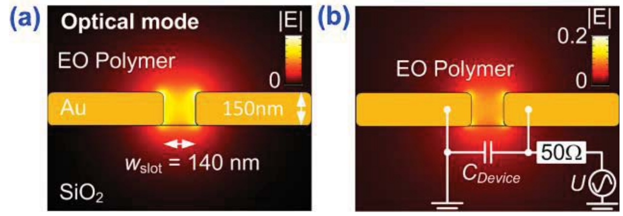

Figure 3: Plasmonic-organic hybrid (POH) phase modulator. **(a)** Optical mode: Light is guided as a surface plasmon polariton (SPP) mode of a metal slot waveguide. The slot is filled with an electro-optic (EO) polymer, and phase modulation is achieved by applying a modulating voltage to the metal sheets. **(b)** RF mode: The applied voltage drops entirely across the slot, leading to perfect overlap with the optical mode in the EO cladding [22].

5. Summary

We have given an overview on our recent progress in the field of silicon-organic hybrid (SOH) and plasmonic-organic hybrid (POH) integration. The concepts combine highly efficient organic electro-optic materials with silicon photonic and plasmonic waveguides, thereby enabling high-performance modulators. We demonstrate the viability of the concepts by realizing highly efficient devices featuring energy consumptions of a few femtojoules per bit, ultra-fast modulators that enable signaling at frequencies of up to 100 GHz, as well as advanced IQ modulators that enable efficient generation of higher-order modulation formats such as QPSK and 16QAM.

We acknowledge support by the European Research Council (ERC Starting Grant 'EnTeraPIC', number 280145), the Alfried Krupp von Bohlen und Halbach Foundation, the EU projects PhoxTroT, BigPipes, Navolchi and SOFI, the Karlsruhe International Research School for Teratronics (HIRST), the Karlsruhe School of Optics and Photonics (KSOP), the Karlsruhe Nano-Micro Facility (KNMF), and the Center for Functional Nanostructures (CFN) of the Deutsche Forschungsgemeinschaft (DFG).

6. References

[1] M. Hochberg, T. Baehr-Jones, "Towards fabless silicon photonics", *Nature Photon.*, vol. 4, no. 8, pp. 492–494, (2010).

[2] G. T. Reed *et al.*, "Silicon optical modulators," *Nature Photon.*, vol. 4, no. 8, pp. 518–526, (2010).

[3] P. Dong *et al.,* "Monolithic silicon photonic integrated circuits for compact 100+ Gb/s coherent optical receivers and transmitters," IEEE J. Sel. Topics Quantum Electron. **20**, 1–8 (2014).

[4] P. Dong, C. Xie, L. Chen, L. Buhl, and Y. Chen, "112-Gb/s monolithic PDM-QPSK modulator in silicon," Opt. Express 20, B624-B629 (2012).

[5] P. Dong *et al.*, "224-Gb/s PDM-16-QAM Modulator and Receiver based on Silicon Photonic Integrated Circuits," in Optical Fiber Communication Conference/National Fiber Optic Engineers Conference 2013, OSA Technical Digest (online) (Optical Society of America, 2013), paper PDP5C.6.

[6] J. Leuthold *et al.* "Plasmonic Communications: Light on a Wire," Opt. Photon. News 24(5), 28-35 (2013).

[7] J. Leuthold *et al.,* "Silicon-organic hybrid electro-optical devices," IEEE J. Sel. Topics Quantum Electron. 19, 114–126 (2013).

[8] L. Alloatti *et al.* "42.7 Gbit/s electro-optic modulator in silicon technology," Opt. Express, vol. 19, no. 12, p. 11841, Jun. 2011.

[9] R. Palmer *et al.*, "Low-Loss Silicon Strip-to-Slot Mode Converters," IEEE Photonics Journal **5**, 2200409 (2013)

[10] R. Palmer *et al.,* "High-speed, low drive-voltage silicon-organic hybrid modulator based on a binary-chromophore electro-optic material," J. Lightw. Technol. 32, 2726–2734 (2014).

[11] L. Alloatti *et al.,* "Optical absorption in silicon layers in the presence of charge inversion/accumulation or ion implantation," Appl. Phys. Lett., vol. 103, no. 5, p. 051104, 2013.

[12] L. Alloatti *et al.,* "100 GHz silicon–organic hybrid modulator," Light Sci. Appl., vol. 3, no. 5, p. e173, May 2014.

[13] R. Palmer *et al.*, "High-Speed Silicon-Organic Hybrid (SOH) Modulator with 1.6 fJ/bit and 180 pm/V In-Device Nonlinearity," *European Conference on Optical Communication* (ECOC 2013), Paper We.3.B.3 (2013).

[14] S. Koeber *et al.,* "Femtojoule Electro-Optic Modulation Using a Silicon-Organic Hybrid Device," Accepted for publication in Light Sci. Appl. (2014)

[15] R. Palmer *et al.*; "Silicon-Organic Hybrid MZI Modulator Generating OOK, BPSK and 8-ASK Signals for up to 84 Gbit/s," *IEEE Photon. J.* **5**, 6600907, (2013).

[16] D. Korn *et al.,* "Silicon-organic hybrid (SOH) IQ modulator using the linear electro-optic effect for transmitting 16QAM at 112 Gbit/s," Opt. Express 21, 13219 (2013).

[17] M. Lauermann *et al.* "16QAM silicon-organic hybrid (SOH) modulator operating with 0.6 V_{pp} and 19 fJ/bit at 112 Gbit/s," in *CLEO: Science and Innovations*, San Jose, California, USA, 2014, p. SM2G.6.

[18] M. Lauermann *et al.* "40 GBd 16QAM modulation at 160 Gbit/s in a silicon-organic hybrid (SOH) modulator," in *40th European Conference on Optical Communication (ECOC 2014)*, France, 2014, p. We.3.1.3.

[19] J. Pfeifle, L. Alloatti, W. Freude, J. Leuthold, and C. Koos, "Silicon-organic hybrid phase shifter based on a slot waveguide with a liquid-crystal cladding," Opt. Express 20, 15359-15376 (2012).

[20] L. Alloatti *et al.*, "Silicon-organic hybrid devices", Proceedings of SPIE 8629, UNSP 86290P (2013)

[21] C. Weimann *et al.,* "Silicon-organic hybrid (SOH) frequency comb sources for terabit/s data transmission," Opt. Express 22, 3629–3637 (2014).

[22] A. Melikyan *et al.,* 'High-speed plasmonic phase modulators,' Nature Photon. 8 (2014) 229–233.

[23] C. Haffner *et al.* 'High-Speed Plasmonic Mach-Zehnder Modulator in a Waveguide', European Conference on Optical Communications (ECOC'2014), Cannes, France; Paper We.3.1.2.